Supplementary Information

Visualization of fast "hydrogen pump" in core-shell nanostructured Mg@Pt through hydrogen stabilized Mg_3Pt

Chong Lu [a,b†], Yanling Ma[a†], Fan Li[a], Hong Zhu[a,d,e], Xiaoqin Zeng [a, b, c], Wenjiang Ding [a, b, c], Jianbo Wu [a,c,e*], Tao Deng[a,c], Jianxin Zou [a, b, c*]

[a] National Engineering Research Center of Light Alloy Net Forming & State Key Laboratory of Metal Matrix Composites, Shanghai Jiao Tong University, Shanghai, 200240, P. R. China

[b] Shanghai Engineering Research Center of Mg Materials and Applications & School of Materials Science and Engineering, Shanghai Jiao Tong University, Shanghai, 200240, P. R. China

[c] Center of Hydrogen Science, Shanghai Jiao Tong University, Shanghai, 200240, P. R. China

[d] University of Michigan – Shanghai Jiao Tong University Joint Institute, Shanghai Jiao Tong University, 800 Dongchuan Road, Shanghai, 200240, P. R.

[e] Materials Genome Initiative Center, Shanghai Jiao Tong University, 800 Dongchuan Road, Shanghai, 200240, P. R.

†these two author contributes equally to this week

Supplementary Figures:

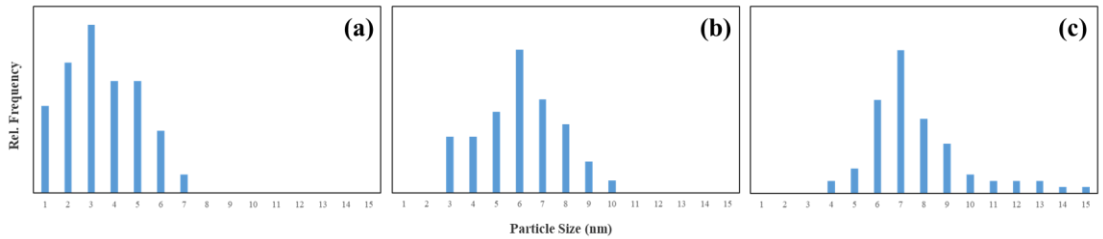

Figure S1. The particle size distributions of Pt particles from as-prepared (a), hydrogenated (b) and dehydrogenated (c) of Mg@Pt composites

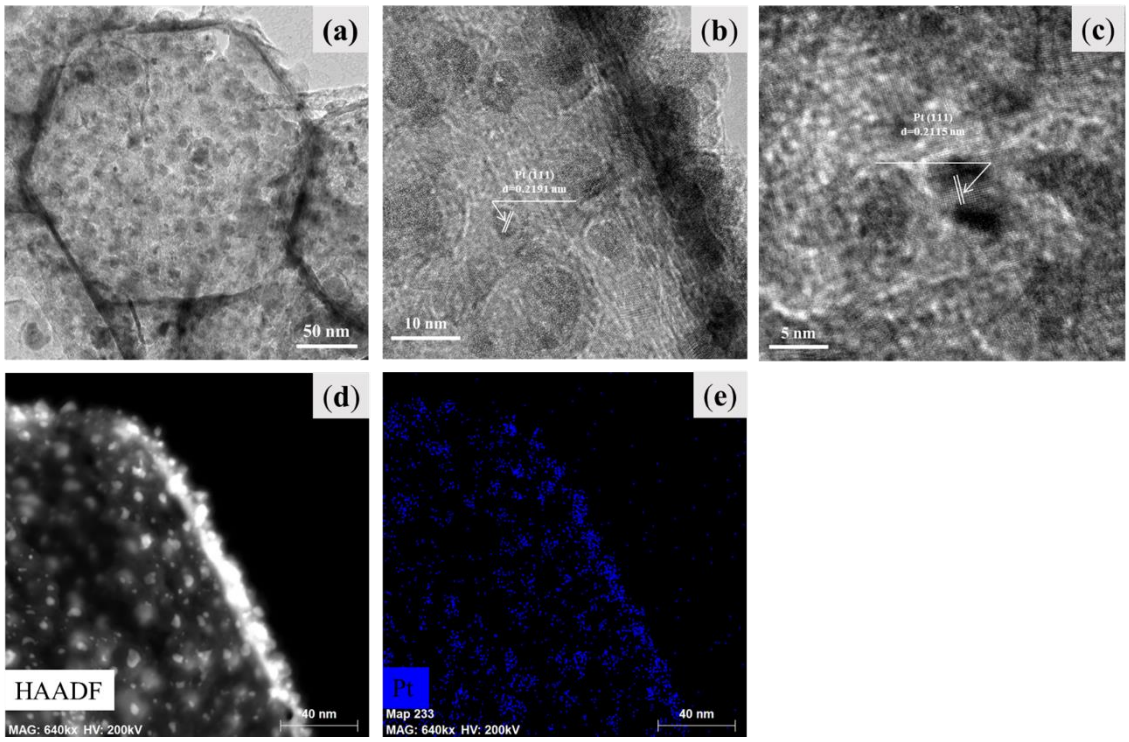

Figure S2. TEM (a), HRTEM (b, c) images, HAADF-STEM (d), the corresponding Pt elements map (e) for dehydrogenated Mg@Pt composites

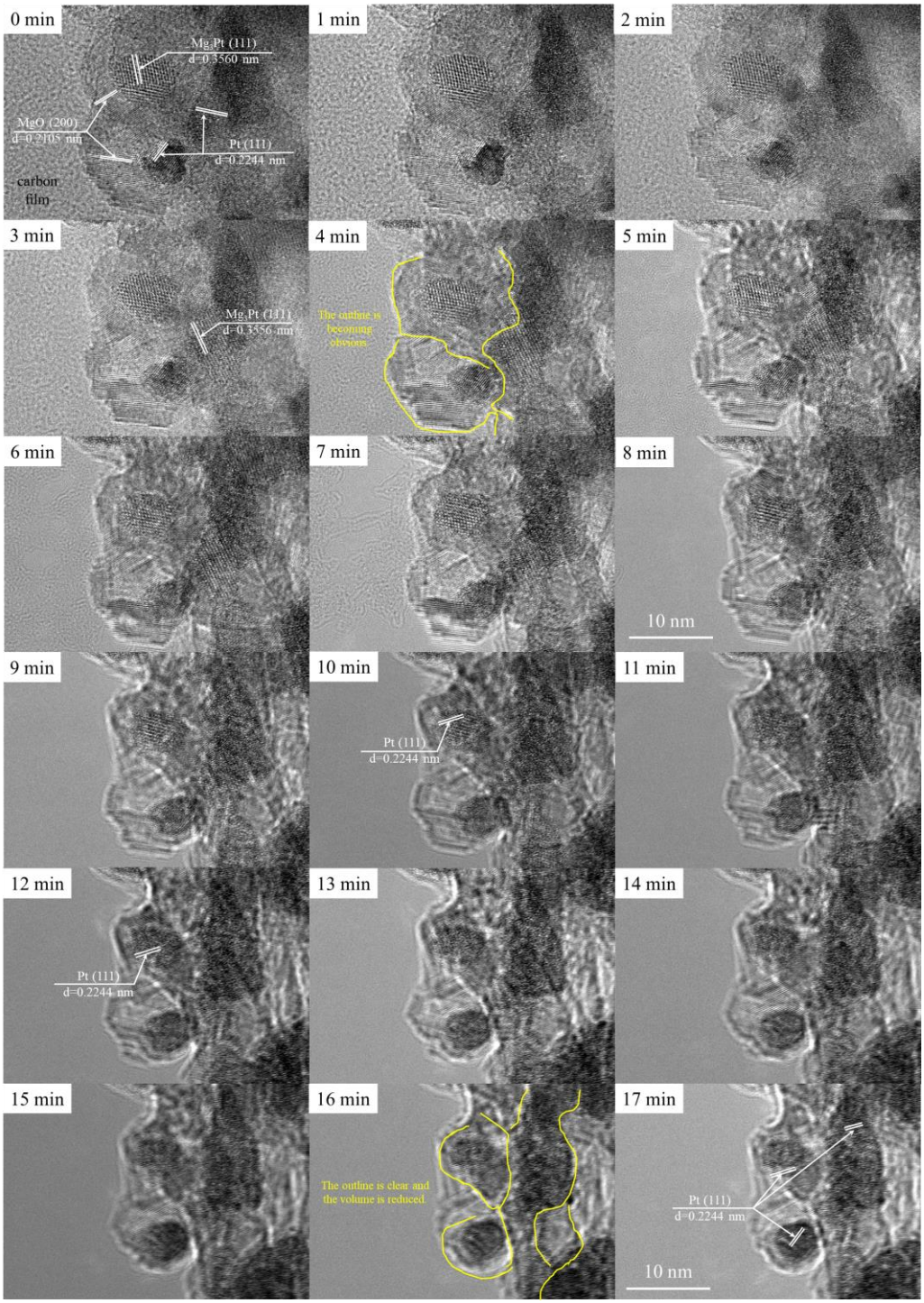

Figure S3. HRTEM images with time under electron radiation during the hydrogen desorption process of for the hydrogenated Mg@Pt composite

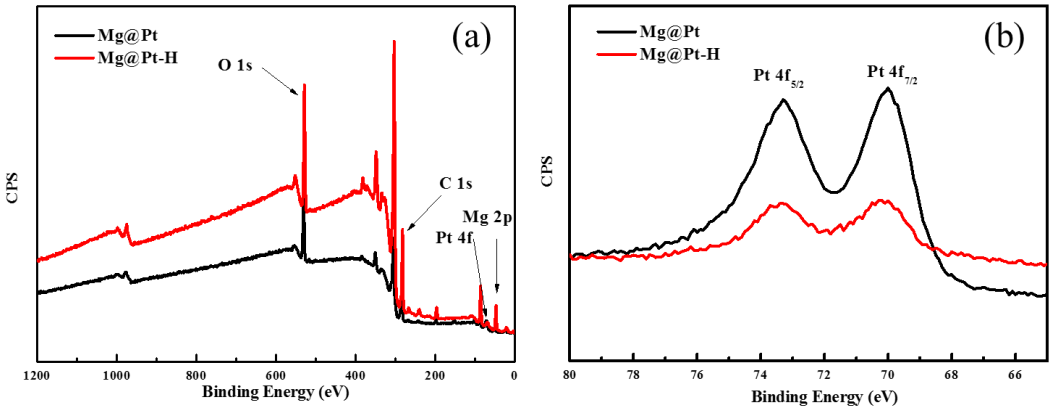

Figure S4. XPS survey scan profiles for the as-prepared and hydrogenated Mg@Pt composites (a) and the corresponding Pt 4f XPS spectra (b)

Supplementary Calculations:

The fitting for calculation of hydrogen sorption activation energy:

According to the Johnson-Mehl-Avrami-Kolmogorov (JMAK) model described as follows[1]:

$$\ln[-\ln(1-\alpha)]=\eta\ln k+\eta\ln t \quad (1),$$

where α is the fraction of Mg transformed into MgH_2 at time t, k is an effective kinetic parameter, and η is the Avrami exponent or reaction order. Based on the experimental data obtained at each measured temperature, the fitted line of $\ln[-\ln(1-\alpha)]$ vs. $\ln t$ can be drawn, where the values of η (the slope) and $\eta\ln k$ (the intercept) can be obtained. According to the values of k at different temperatures, the E_a for Mg and Mg@Pt can be approximately acquired from the Arrhenius equation:

$$k=A\exp(-E_a/RT) \quad (2),$$

where A is a temperature-independent coefficient, R is the universal gas constant (8.314 J mol^{-1} K^{-1}), and T is the absolute temperature. It should be noted that JMAK model is used under the circumstance that a saturated value for hydrogen absorption or desorption is achieved [1]. In our case, some hydrogen absorption/desorption profiles obtained at relatively low temperatures, i.e., absorption at 200°C and desorption at 300°C for pure Mg, absorption at 200°C and desorption at 275°C for Mg@Pt, do not have a saturation point under current measurement conditions and are therefore not considered for the determination of activation energies using the JMAK model. Consequently, the corresponding data points in Figs. 2(e) and 2(f) are absent.

The calculation condition for defect formation energy:

In view of the interstitial H atom, the ratio of Mg and Pt is always 3 : 1, thus there is no need to calculate the individual potential of Mg and Pt. The known value for formation energy of Mg_3Pt is 601 meV^2, which can be got as follows:

$$E_{f(Mg3Pt)} = E_{Mg3Pt} - 3\mu_{Mg} - \mu_{Pt} \quad (3),$$

where $E_{f(Mg3Pt)}$ is the formation energy of Mg_3Pt and E_{Mg3Pt} is the energy of the perfect Mg_3Pt crystal. With these two formulas provided, E_f can be simplified to:

$$E_f(T, p) = E_{Mg3Pt-H} - E_{Mg3Pt} - E_{f(Mg3Pt)} - \mu_H(T, p) \quad (4).$$

With regard to the chemical potential of H atom at finite temperature and pressure, we can calculate it as follows:

$$\mu_H(T, p) = 1/2\mu_{H2}(T, p) = 1/2\mu_{H2}(T, p^o) + 1/2kT\ ln(p_{H2}/\ p^o_{H2}) \quad (5),$$

where $\mu_H(T, p)$ and $\mu_{H2}(T, p)$ are the H and H_2 chemical potential at finite temperature and pressure, respectively. $\mu_{H2}(T, p^o)$ is the chemical potential of hydrogen at one particular pressure, p_{H2} is the pressure of hydrogen and p^o_{H2} is the particular pressure of hydrogen. Selecting the zero-reference state of $\mu_{H2}(0K, p^o)$ as a reference. $\mu_{H2}(T, p^o)$ is given using the equation G = H − TS between the Gibbs free energy, G, and the enthalpy, H, as follows:

$$\mu_{H2}(T, p^o) = \mu_{H2}(0K, p^o) + \Delta G(\Delta T, p^o, H_2) = \mu_{H2}(0K, p^o) + (H(T, p^o, H_2) - H(0K, p^o, H_2)) - T(S(T, p^o, H_2) - S(0K, p^o, H_2)) \quad (6),$$

where we can search these related values in the JANAF thermochemical for standard pressure, p^o = 1 atm. Therefore, we can obtain the aspired temperature dependence simply from the differences in the enthalpy and entropy, S, of an H_2 molecule with respect to the T = 0 K limit.

Supplementary Table:

Table S1. Hydrogen sorption properties of some Mg-based alloys and composites.

Composites	Hydrogen Content (wt% H_2)	Hydrogen Sorption Activation Energy (kJ/mol H_2)		Ref
		hydrogenation	dehydrogenation	
$CaMg_{1.9}Ni_{0.1}$	5.65	41.7	/	3
Mg_3Pr	2.58	/	/	4
Melt-spun $Mg_{90}Ce_5Ni_5$	5.3	/	109.2	5
Mg-5wt%Gd	5.7	/	149	6
$Mg_{17}Ba_2$	4.0	/	173.9	7
ultrafine Mg	7.1	110.9	152.6	this study
Mg@Pt	6.5	84.3	152.8	this study

Table S2. The element compositions obtained from line scanning analysis inserted in Fig. 3 (b4).

Elements	Atom (at %)
Magnesium (Mg)	76.30
Platinum (Pt)	23.67

Table S3. Analysis of bond length before and after H doping in the tetrahedral site and octahedral site, respectively.

Atom1	Atom2	tetrahedral site		octahedral site	
		L_{ini} (Å)	L_{dop} (Å)	L_{ini} (Å)	L_{dop} (Å)
Mg1	**Mg2**	2.98813	3.10444	3.0189	3.03865
Mg2	**Mg3**	3.0668	3.21168	3.1065	3.21718
Mg3	**Pt**	2.69813	2.76082	2.77529	2.76948
Pt	**Mg1**	2.77529	2.8309	3.4182	3.50244

Notes: L_{ini}: the bond length before H doping, L_{dop} (Å): the bond length after H doping.

Supplementary Reference

1. M. Fanfoni, M. Tomellini, *IL Nuovo Cimento,* 1998; **20**: 1171-1182.

2. De Jong M, Chen W, Angsten T, et al., *Scientific data*, 2015; **2**: 150009

3. M. Ma, R. Duan, L.Z. Ouyang, et al., *J. Alloys Compd.*, 2017, **691**, 929-935.

4. L.Z. Ouyang, X.S. Yang, H.W. Dong, et al., *Scripta Mater.*, 2009, **61**, 339-342.

5. H.J. Lin, L.Z. Ouyang, H. Wang, et al., *Int. J. Hydrogen Energy*, 2012, **37**, 14329-14335.

6. D. Wu, L.Z. Ouyang, C. Wu, et al., *J. Alloys Compd.*, 2015, **642**, 180-184.

7. D. Wu, L.Z. Ouyang, C. Wu, et al., *J. Alloys Compd.*, 2017, **690**, 519-522.